IscU as a Scaffold for Iron−Sulfur Cluster Biosynthesis: Sequential Assembly of [2Fe-2S] and [4Fe-4S] Clusters in IscU†

Jeffrey N. Agar,‡ Carsten Krebs,§ Jeverson Frazzon,|| Boi Hanh Huynh,§ Dennis R. Dean,*,|| and Michael K. Johnson*,‡

Department of Chemistry and Center for Metalloenzyme Studies, University of Georgia, Athens, Georgia 30602, Department of Biochemistry, Virginia Tech, Blacksburg, Virginia 24061, and Department of Physics, Emory University, Atlanta, Georgia 30322

Received April 25, 2000; Revised Manuscript Received May 24, 2000

ABSTRACT: Iron−sulfur cluster biosynthesis in both prokaryotic and eukaryotic cells is known to be mediated by two highly conserved proteins, termed IscS and IscU in prokaryotes. The homodimeric IscS protein has been shown to be a cysteine desulfurase that catalyzes the reductive conversion of cysteine to alanine and sulfide. In this work, the time course of IscS-mediated Fe−S cluster assembly in IscU was monitored via anaerobic anion exchange chromatography. The nature and properties of the clusters assembled in discrete fractions were assessed via analytical studies together with absorption, resonance Raman, and Mössbauer investigations. The results show sequential cluster assembly with the initial IscU product containing one $[2Fe\text{-}2S]^{2+}$ cluster per dimer converting first to a form containing two $[2Fe\text{-}2S]^{2+}$ clusters per dimer and finally to a form that contains one $[4Fe\text{-}4S]^{2+}$ cluster per dimer. Both the $[2Fe\text{-}2S]^{2+}$ and $[4Fe\text{-}4S]^{2+}$ clusters in IscU are reductively labile and are degraded within minutes upon being exposed to air. On the basis of sequence considerations and spectroscopic studies, the $[2Fe\text{-}2S]^{2+}$ clusters in IscU are shown to have incomplete cysteinyl ligation. In addition, the resonance Raman spectrum of the $[4Fe\text{-}4S]^{2+}$ cluster in IscU is best interpreted in terms of noncysteinyl ligation at a unique Fe site. The ability to assemble both $[2Fe\text{-}2S]^{2+}$ and $[4Fe\text{-}4S]^{2+}$ clusters in IscU supports the proposal that this ubiquitous protein provides a scaffold for IscS-mediated assembly of clusters that are subsequently used for maturation of apo Fe−S proteins.

Iron−sulfur clusters are ubiquitous in nature and exhibit diverse functions which include mediating electron transport, providing the active sites of redox and nonredox enzymes, acting as sensors for regulatory processes, and generating organic radicals to initiate radical reactions (*1*−*4*). While the past two decades have witnessed a proliferation of data concerning the structure−function relationships of Fe−S clusters, the detailed mechanism of Fe−S cluster biosynthesis has remained elusive. Much of what is currently known stems from investigations into the function of specific genes involved with nitrogen fixation in *Azotobacter vinelandii*. Two gene products, NifS and NifU, have been extensively characterized and found to be essential for full activation and cluster assembly in both nitrogenase component proteins (*5*−*11*).

On the basis of sequence homology with the *nif* genes that specifically target nitrogenase Fe−S cluster biosynthesis, an *isc* (iron−sulfur cluster) gene cluster was identified in a wide range of nitrogen-fixing and non-nitrogen-fixing prokaryotes and proposed to be responsible for general Fe−S cluster biosynthesis (*12*). Two of the nine *isc* genes, *iscS* and *iscU*, encode homodimeric proteins whose sequences are homologous to NifS and NifU, respectively. Furthermore, in common with NifU and NifS (*11*), the gene products IscU and IscS have been shown to produce a heterotetrameric complex (*12*). IscS was purified from *Escherichia coli* and *A. vinelandii* and shown to be a pyridoxal phosphate-dependent L-cysteine desulfurase closely related to NifS (*13*, *14*). Recently, X-ray crystal structures of two members of this general class of enzyme have appeared (*15*, *16*), and the active site structures are in good agreement with previous mechanistic proposals involving an active site cysteine persulfide intermediate (*8*). IscU corresponds to the N-terminal domain of NifU and contains three conserved cysteine residues [Cys^{37}, Cys^{63}, and Cys^{106} in *A. vinelandii* and *E. coli* IscU (*13*)]. In accord with the notion that Fe−S clusters are among the most ancient types of prosthetic group, the Isc proteins, in general, and IscU and IscS, in particular, have been widely conserved throughout evolution. Indeed, IscU is widely considered to be one of the most conserved protein sequences in nature (*17*). Moreover, in the past two years, proteins homologous to the prokaryotic *iscS* and *iscU*

† This work was supported by the National Science Foundation (Grant MCB9630127 to D.R.D.), by the National Institutes of Health (Grant GM51962 to M.K.J. and Grant GM47295 to B.H.H.), and by a National Science Foundation Research Training Group Award to the Center for Metalloenzyme Studies (DBI9413236).

* To whom correspondence should be addressed. M.K.J.: Department of Chemistry, University of Georgia, Athens, GA 30602; telephone, (706) 542-9378; fax, (706) 542-2353; e-mail, johnson@chem.uga.edu. D.R.D.: Department of Biochemistry, Virginia Tech, Blacksburg, VA 24061; telephone, (540) 231-5895; fax, (540) 231-7126; e-mail, deandr@vt.edu.

‡ Univeristy of Georgia.

§ Emory University.

|| Virginia Tech.

10.1021/bi000931n CCC: $19.00
Published on Web 06/14/2000

gene products have been shown to be involved in Fe−S cluster assembly in eukaryotic organisms (*18*−*21*), on the basis of both biochemical and genetic evidence. Hence, understanding the function of the IscU and IscS proteins in prokaryotes is likely to provide insight into iron homeostasis and Fe−S cluster assembly in mitochondria, with potential relevance to iron-storage diseases and the control of cellular iron uptake.

The absence of a permanent [2Fe-2S] cluster in IscU and the enhanced stability of transient clusters assembled in IscU compared to the stability of those in NifU make IscU an attractive system for investigating further the putative role of this protein as a scaffold for Fe−S cluster biosynthesis. Support for this role has come from our recent studies which demonstrated IscS-mediated assembly of one reductively labile $[2Fe\text{-}2S]^{2+}$ cluster per dimer in *A. vinelandii* IscU (*12*). In the work presented here, we report a detailed investigation of the time course of IscS-mediated cluster assembly in *A. vinelandii* IscU using preparative FPLC to separate fractions and the combination of analytical, absorption, Mössbauer, and resonance Raman studies to establish the number, type, and properties of clusters in discrete fractions.

MATERIALS AND METHODS

A. vinelandii IscS and IscU were heterologously produced in *E. coli* and purified as previously described (*12*, *13*). IscS-mediated cluster assembly experiments, including time-based separation of discrete fractions using a Pharmacia FPLC system and the preparation of all spectroscopic samples, were carried out under rigorously anaerobic conditions inside a Vacuum Atmospheres glovebox under an Ar atmosphere (<1 ppm O_2). Typical experiments involved initiating cluster biosynthesis by addition of 4 mM L-cysteine to a reaction mixture containing 100−400 μM IscU in the presence of 0.5−5.0 μM IscS, a 5-fold excess of freshly prepared ferric ammonium citrate (relative to the IscU concentration), and 4 mM β-mercaptoethanol. The rate of cluster assembly was controlled by varying the IscU:IscS ratio, and ^{57}Fe-enriched ferric ammonium citrate (>95% enrichment) was used whenever Mössbauer samples were to be prepared. At selected time intervals, samples were loaded onto an 8 mL mono-Q column (Pharmacia) and eluted with a shallow 0.1 to 0.4 M NaCl gradient. Individual fractions were concentrated and desalted via ultrafiltration prior to spectroscopic studies. All spectroscopic and cluster assembly studies were carried out in 50 mM Tris-HCl buffer (pH 7.8). Concentrations are based on IscU monomer (MW = 13 742 for the apoprotein) and were assessed by protein determinations carried out after trichloroacetic acid precipitation and redissolution using the BCA method (*22*). Iron analyses were conducted colorimetrically on dithionite-treated samples using the ferrous ion chelator α,α′-*N*-dipyridyl (ϵ_{520} = 8.4 mM^{-1} cm^{-1}).

UV−visible absorption spectra were recorded under anaerobic conditions in septum-sealed 1 mm and 1 cm cuvettes, using a Shimadzu 3101PC scanning spectrophotometer fitted with a TCC-260 temperature controller. Resonance Raman spectra were recorded on droplets of frozen protein solutions at 17 K using an Instruments SA Ramanor U1000 scanning spectrometer fitted with a cooled RCA 31034 photomultiplier tube and lines from a Coherent Sabre 10-W argon ion laser. Mössbauer spectra in the presence of weak and strong applied magnetic fields were recorded using the previously described instrumentation (*23*), and specific experimental conditions are given in the figure legend. Analysis of the Mössbauer data was performed with the program WMOSS (WEB Research).

RESULTS

FPLC and UV−Visible Absorption Analysis of the Time Course of IscS-Mediated Cluster Assembly in IscU. Our previous studies on IscS-mediated cluster assembly in IscU under strictly anaerobic conditions revealed the progressive development of a $[2Fe\text{-}2S]^{2+}$ chromophore over a period of approximately 1 h. These experiments involved a reaction mixture comprising IscU with 0.5−8 equiv of ferric ammonium citrate, catalytic amounts of IscS (70:1 IscU:IscS ratio), and excess β-mercaptoethanol, and initiating the reaction by addition of excess L-cysteine. On the basis of visible extinction coefficients and Fe quantitation of EDTA-treated samples, it was concluded that one $[2Fe\text{-}2S]^{2+}$ cluster was assembled per IscU dimer under these conditions. However, monitoring cluster assembly in IscU by UV−visible absorption over longer time periods was impeded due to the concomitant formation of iron sulfides. Consequently, a more detailed investigation of the time course of cluster assembly in IscU was undertaken using anaerobic FPLC with a mono-Q column and a 0.1 to 0.4 M NaCl gradient to separate fractions contained in samples taken from the reaction mixture at discrete time intervals. Mono-Q columns are capable of separating fractions with small conformation differences and have been shown to be effective in separating fractions of specific Fe−S proteins that differ in terms of cluster type or stoichiometry (*24*). The results of two sets of FPLC experiments in which protein absorbance at 280 nm was monitored at selected times during IscS-mediated cluster assembly in IscU are shown in Figure 1.

In the first FPLC experiment (Figure 1A), the IscU:IscS ratio was increased to 460:1 to slow the reaction and thereby afford temporal resolution of IscU species that cannot be observed in 1:1 mixtures. The level of the IscU apoprotein (fraction 1) that dominates prior to L-cysteine addition (0 h) progressively decreases as the reaction proceeds with a concomitant increase in the level of fraction 2 (2.5 h). No apoprotein is observed after 6.5 h, but a new fraction (fraction 3) starts to appear and is the dominant form of IscU after 7.5 h. Iron and protein analyses indicated 1.2 and 1.9 Fe molecules/IscU monomer, for fractions 2 and 3, respectively. These values are likely to be an overestimate for fraction 2 and an underestimate for fraction 3 due to the difficulty in obtaining baseline separation of fractions 2 and 3. The UV−visible absorption spectra of fractions 2 and 3 are both characteristic of $[2Fe\text{-}2S]^{2+}$ centers (Figure 2), with the former corresponding to that reported previously for IscU samples containing one $[2Fe\text{-}2S]^{2+}$ cluster per IscU dimer (*12*). In accord with the Fe analyses, comparison of the visible extinction coefficients (ϵ_{456} = 5.8 and 9.2 mM^{-1} cm^{-1} for fractions 2 and 3, respectively) and the A_{456}/A_{280} ratios (0.31 and 0.44 for fractions 2 and 3, respectively) with well-characterized $[2Fe\text{-}2S]^{2+}$-containing proteins (*25*) (after correction of the 280 nm absorbance for the one W and four Y residues per IscU monomer) shows that fractions 2 and 3

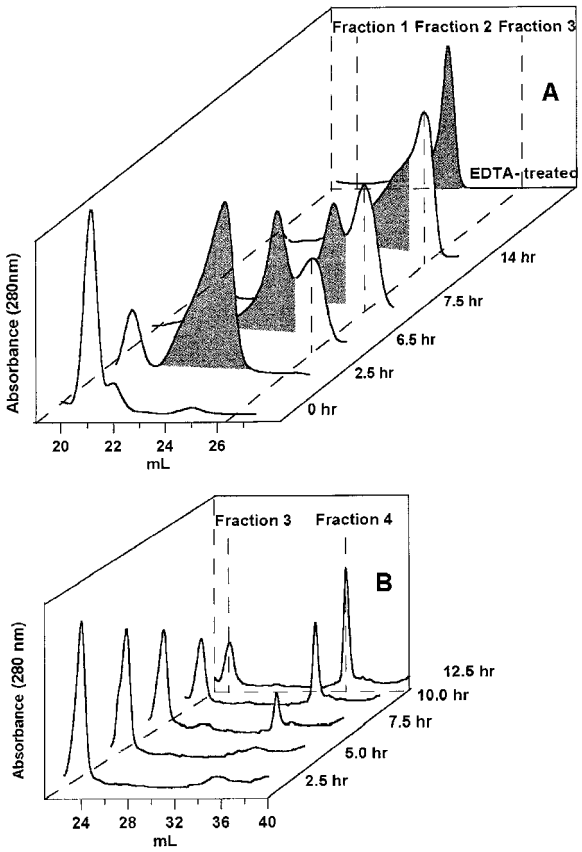

FIGURE 1: Anaerobic FPLC analysis of the reaction mixture during IscS-mediated cluster assembly in IscU. Samples taken at selected time intervals after addition of 4 mM L-cysteine to the reaction mixture were loaded on a mono-Q column, eluted with a 0.1 to 0.4 M NaCl gradient, and monitored by absorption at 280 nm. Each trace is aligned in a stack plot based on the conductivity of the eluting fraction. (A) Reaction mixture containing 370 μM IscU, 0.8 μM IscS, 1.85 mM ferric ammonium citrate, and 4 mM β-mercaptoethanol. Conductivity range of 156−193 mM NaCl. The trace labeled EDTA-treated corresponds to a sample in which fractions 2 and 3 were combined and treated with a 20-fold excess of EDTA for 10 min before being reloaded onto the column. (B) Reaction mixture containing 140 μM IscU, 5.0 μM IscS, 0.7 mM ferric ammonium citrate, and 4 mM β-mercaptoethanol. Conductivity range of 131−350 mM NaCl.

contain one and two $[2Fe\text{-}2S]^{2+}$ clusters per IscU dimer, respectively.

Because our previous studies showed that IscU samples containing one $[2Fe\text{-}2S]^{2+}$ cluster per IscU dimer were stable to EDTA treatment (*12*), fractions 2 and 3 were combined, treated with a 20-fold excess of EDTA for 10 min, and repurified by FPLC. The resulting sample contained only fraction 2 (Figure 1A), thereby providing homogeneous samples of IscU containing one $[2Fe\text{-}2S]^{2+}$ cluster per dimer for spectroscopic investigations. The absorption spectrum of the EDTA-treated sample (Figure 2) has an ϵ_{456} of 4.6 mM^{-1} cm^{-1} and an A_{456}/A_{280} of 0.27, in good agreement with our previous results (*12*). We conclude that forms of IscU with two $[2Fe\text{-}2S]^{2+}$ clusters per dimer can be prepared, but that one cluster is readily removed by Fe chelators.

In the second FPLC experiment (Figure 1B), the IscU:IscS ratio was decreased from 460:1 to 28:1. Under these conditions, IscU containing two $[2Fe\text{-}2S]^{2+}$ clusters per dimer (fraction 3) is the dominant species after 2.5 h. However, over the next 10 h, the level of this fraction decreases with

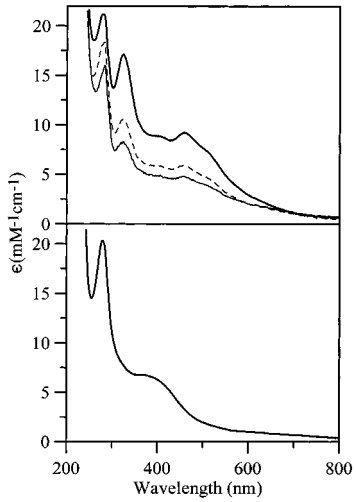

FIGURE 2: UV−visible absorption spectra of Fe−S cluster-containing IscU samples: (top) fraction 2 (dashed line), fraction 3 (thick line), and EDTA-treated sample (thin line) and (bottom) fraction 4. The samples are described in the legend of Figure 1.

a concomitant increase in the level of a new fraction (fraction 4). The UV−visible absorption spectrum of fraction 4 (Figure 2) comprises a broad absorption centered at ~390 nm and is characteristic of a $[4Fe\text{-}4S]^{2+}$ cluster (*25*). Iron and protein analyses for fraction 4 revealed 1.9 Fe molecules/IscU monomer. Moreover, the visible extinction coefficient ($\epsilon_{390} = 7.4$ mM^{-1} cm^{-1}) and the A_{390}/A_{280} ratio (0.34), when compared to those of well-characterized $[4Fe\text{-}4S]^{2+}$-containing proteins (*26*, *27*) after correction for the number of 280 nm-absorbing W and Y residues in IscU, are indicative of one $[4Fe\text{-}4S]^{2+}$ cluster per IscU dimer. Subsequent FPLC experiments with a 1:1 IscU:IscS ratio showed that the IscS-mediated cluster assembly reaction proceeds rapidly to yield only the $[4Fe\text{-}4S]^{2+}$-containing fraction in less than 1 h.

UV−visible absorption studies showed that the Fe−S chromophores present in IscU fractions 2−4 were irreversibly and completely degraded within minutes after exposure to air or immediately upon anaerobic addition of a 10-fold excess of dithionite. Moreover, EPR spectra of samples frozen within 2 s of dithionite addition did not reveal any resonances indicative of paramagnetic $[2Fe\text{-}2S]^{+}$ or $[4Fe\text{-}4S]^{+}$ clusters. Consequently, resonance Raman and Mössbauer studies were carried out to confirm cluster type and assess cluster ligation.

Resonance Raman Characterization of $[2Fe\text{-}2S]^{2+}$ Centers Assembled in IscU. The resonance Raman spectra of fractions 2 and 3 in the Fe−S stretching region (Figure 3) are identical within experimental error and indicative of $[2Fe\text{-}2S]^{2+}$ centers. Hence, the two $[2Fe\text{-}2S]^{2+}$ clusters in fraction 3 and the single $[2Fe\text{-}2S]^{2+}$ cluster in fraction 2 must all have very similar environments. The spectra are in good agreement with those previously reported and assigned for $[2Fe\text{-}2S]^{2+}$-containing IscU using 457 nm excitation (*12*). The only significant differences compared to previously published spectra are decreased intensity, improved resolution, and 3 cm^{-1} downshifts for the bands in the 340−370 nm region. Since the IscU samples in these initial resonance Raman studies were used without chromatographic separation of discrete fractions, these differences are readily interpreted in terms of contributions from the $[4Fe\text{-}4S]^{2+}$-containing form of IscU (fraction 4).

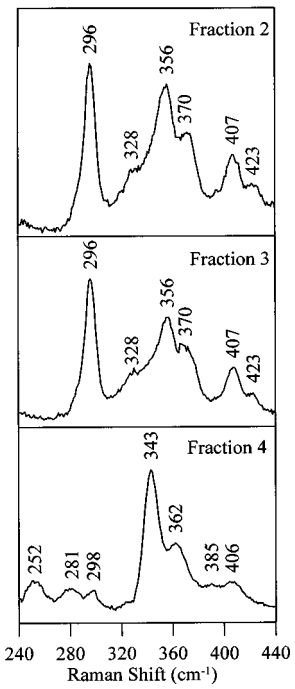

FIGURE 3: Low-temperature resonance Raman spectra of Fe−S cluster-containing IscU samples. The samples corresponding to fractions 2−4 are described in the legend of Figure 1 and were concentrated to ~2 mM in IscU monomer prior to freezing a 10 μL droplet on the coldfinger of a Displex unit at 17 K. The spectra were recorded using 457 nm excitation with 100 mW of laser power at the sample. Each spectrum is the sum of 100 scans, with each scan involving photon counting for 1 s at 1 cm^{-1} increments, with 6 cm^{-1} resolution. Bands due to lattice modes of the frozen buffer solution have been subtracted from all spectra.

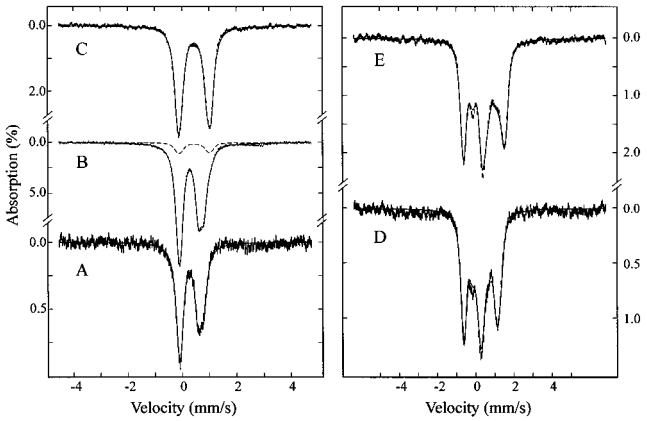

FIGURE 4: Mössbauer spectra of Fe−S cluster-containing IscU samples: fraction 2 (A and D), corresponding to the EDTA-treated sample as described in the legend of Figure 1; fraction 3 (B); and fraction 4 (C and E). The samples are described in the legend of Figure 1 and were concentrated by anaerobic centricon ultrafiltration at room temperature to 0.41−2.2 mM in IscU monomer, before being loaded into Mössbauer sample holders. The spectra were recorded at 4.2 K in a field of 50 mT (A−C) or 4 T (D and E) applied parallel to the γ-beam. The dashed line in part B is spectrum C normalized to 10% of the total absorption area of spectrum B. The solid lines are either least-squares fits or theoretical simulations, as described in the text.

As previously noted (*12*), the resonance Raman characteristics of the $[2Fe\text{-}2S]^{2+}$ center in IscU can be interpreted in terms of either complete cysteinyl ligation or partial noncysteinyl ligation. However, since the results presented herein show that two $[2Fe\text{-}2S]^{2+}$ clusters can be assembled per IscU dimer and each subunit contains only three cysteine residues, each cluster can maximally have three cysteine ligands. The frequencies of the A_g^t and B_{3u}^t predominantly Fe−S(Cys) stretching modes of biological $[2Fe\text{-}2S]^{2+}$ clusters generally provide an indication of cluster ligation (*28*). For the $[2Fe\text{-}2S]^{2+}$ cluster in IscU, these bands occur at anomalously high frequencies (356 and 296 cm^{-1}, respectively) compared to those of the all-cysteine-ligated $[2Fe\text{-}2S]^{2+}$ clusters in ferredoxins (281−291 and 326−340 cm^{-1}, respectively), but within the ranges established for $[2Fe\text{-}2S]^{2+}$ clusters with one serinate ligand introduced via site-directed mutagenesis (332−356 and 289−302 cm^{-1}, respectively) (*28*). Currently, the only known exception is the all-cysteinyl-ligated $[2Fe\text{-}2S]^{2+}$ cluster in human ferrochelatase which has the A_g^t and B_{3u}^t Fe−S(Cys) stretching modes at 350 and 295 cm^{-1}, respectively (*28*). In this case, the recent X-ray crystal structure indicates that the anomalous high frequencies of these modes are a consequence of dramatic differences in hydrogen-bonding interactions and cysteinyl $Fe-S_\gamma-C_\beta-C_\alpha$ dihedral angles compared to those of ferredoxins (*29*). The resonance Raman data provide only limited information about the number or nature of the noncysteinyl [2Fe-2S] cluster ligands in IscU. However, the Raman spectra argue against ligation by the side chains of a histidyl and tyrosyl residues. On the basis of studies of a Rieske protein (*30*), histidyl ligation would be expected to decrease Fe−S(Cys) stretching frequencies due to the larger effective mass of the imidazole ring, and the characteristic Fe^{3+}−tyrosinate vibrational modes (*31*) are not observed. Water/OH^-, serinate, aspartate, and glutamate are the best candidates for oxygenic ligation, although nitrogenic ligation from lysine or the N-terminal amino group cannot be ruled out.

Mössbauer Characterization of the $[2Fe\text{-}2S]^{2+}$ Centers Assembled in IscU. Direct evidence for at least partial noncysteinyl ligation at one of the Fe sites of the $[2Fe\text{-}2S]^{2+}$ clusters in IscU was provided by Mössbauer spectroscopy. Parts A and B of Figure 4 show the 4.2 K Mössbauer spectra recorded in the presence of a weak magnetic field of 50 mT for samples of IscS-reconstituted IscU corresponding to fractions 2 and 3, respectively. The fraction 2 sample corresponds to the EDTA-treated sample described above and characterized by FPLC and absorption in Figures 1 and 2, respectively. The fraction 3 sample contained some unresolved fraction 2, and FPLC analysis of the concentrated sample used for Mössbauer analysis indicated ~60% of the two $[2Fe\text{-}2S]^{2+}$ clusters per dimer form (fraction 3), ~30% of the one $[2Fe\text{-}2S]^{2+}$ cluster per dimer form (fraction 2), and ~10% of the one $[4Fe\text{-}4S]^{2+}$ cluster per dimer form (fraction 4). The latter presumably formed during the concentration step. The Mössbauer spectra of both samples are very similar and comprise two partially resolved quadrupole doublets.

The spectrum of fraction 2 (Figure 4A) can be least-squares fitted with two quadrupole doublets of equal intensity, indicating the presence of two iron sites with equal concentration but different coordination environments. The results of the fits are plotted as a solid line overlaid with the experimental spectrum (Figure 4A). The parameters obtained for both Fe sites (Table 1) are typical for high-spin ferric ions. The smaller isomer shift, 0.26 mm/s, determined for site 1 is indicative of tetrahedral sulfur coordination (*32*), while the larger isomer shift, 0.32 mm/s, obtained for site 2

Table 1: Mössbauer Parameters at 4.2 K for the Fe−S Clusters Assembled in IscU

sample	cluster type	Fe site	δ (mm/s)	ΔE_Q (mm/s)	η
fraction 2[a]	$[2Fe\text{-}2S]^{2+}$	1	0.26 ± 0.03	0.64 ± 0.05	1.0
		2	0.32 ± 0.03	0.91 ± 0.05	0.7
fraction 3[b]	$[2Fe\text{-}2S]^{2+}$	1	0.27 ± 0.02	0.66 ± 0.04	1.0
		2	0.32 ± 0.02	0.94 ± 0.04	0.7
fraction 4	$[4Fe\text{-}4S]^{2+}$	pair 1[c]	0.44 ± 0.02	0.98 ± 0.04	0.3
		pair 2[c]	0.45 ± 0.02	1.23 ± 0.04	0.7

[a] Homogeneous fraction 2 prepared by EDTA treatment of a combined sample of fractions 2 and 3 as described in the text. [b] On the basis of FPLC and Mössbauer analysis of this sample, fractions 3, 2, and 4 contribute 71, 18, and 11% to the total Mössbauer absorption, respectively. See the text for further details. [c] $[4Fe\text{-}4S]^{2+}$ clusters may be considered to comprise two valence-delocalized Fe(II)Fe(III) pairs.

suggests the presence of non-sulfur ligands (*33*). The fact that these two high-spin ferric sites exhibit quadrupole-doublet spectra at 4.2 K suggests that either they are associated with an integer-spin system or their electronic relaxations are fast in comparison with the ^{57}Fe nuclear Larmor precession. The latter is rare for high-spin ferric ions at 4.2 K. To distinguish these two situations, we have recorded the spectrum of fraction 2 at 4.2 K in a parallel applied field of 4 T (Figure 4D). The solid line plotted over the experimental spectrum is a theoretical simulation using the parameters determined for the two doublets and assuming diamagnetism. The agreement between the simulation and experiment indicates that the two iron sites are indeed associated with a diamagnetic system. For the all-ferric Fe−S clusters, diamagnetism is unique to the $[2Fe\text{-}2S]^{2+}$ cluster, of which the two ferric ions are antiferromagnetically coupled to form a diamagnetic ground state (*34*). Consequently, the Mössbauer data presented above confirm that the EDTA-treated IscU sample contains only $[2Fe\text{-}2S]^{2+}$ clusters and indicate the presence of noncysteinyl ligation at one of the iron sites. The only crystallographically defined biological $[2Fe\text{-}2S]^{2+}$ center with noncysteinyl ligation that has been characterized by Mössbauer spectroscopy is the Rieske protein which has two histidyl ligands on one Fe site (*33*, *35*). Within experimental uncertainties, the Mössbauer parameters obtained for the $[2Fe\text{-}2S]^{2+}$ cluster in IscU are identical to those of the $[2Fe\text{-}2S]^{2+}$ cluster of the Rieske protein (*33*). However, the Mössbauer parameters for the noncysteinyl ligated site are not expected to be sensitive to O or N ligation. Hence, although the resonance Raman data and the lack of two conserved histidine residues in IscU (*13*) argue strongly against a histidyl-ligated Rieske-type center, the Mössbauer data dictate one or two noncysteinyl ligands at one Fe site of the $[2Fe\text{-}2S]^{2+}$ cluster in IscU.

Comparison of panels A and B of Figure 4 shows that the Mössbauer spectra of the forms of IscU with one and two $[2Fe\text{-}2S]^{2+}$ clusters per dimer are the same within experimental error. The only significant difference in the Mössbauer spectra of these samples is a shoulder at ~ 1 mm/s in the predominantly fraction 3 sample (Figure 4B). The position of this shoulder coincides with that of the high-energy line of the $[4Fe\text{-}4S]^{2+}$ cluster that is present in fraction 4 (Figure 4C; see below). Therefore, in accord with the FPLC data, analysis of the Mössbauer spectrum indicates that approximately 10% of the iron absorption can be attributed to a $[4Fe\text{-}4S]^{2+}$ cluster that must have formed during concentration of the sample. The dashed line plotted in Figure 4B is the spectrum of the $[4Fe\text{-}4S]^{2+}$ cluster in fraction 4 normalized to 10% absorption of the experimental spectrum. Removal of this contribution of the $[4Fe\text{-}4S]^{2+}$ cluster from the raw data yielded a spectrum that can be fitted with two quadrupole doublets of equal intensity. Within experimental errors, the parameters obtained from the fit (listed in Table 1) are identical to those of the $[2Fe\text{-}2S]^{2+}$ cluster in fraction 2. The solid line plotted over spectrum B is generated by addition of the $[4Fe\text{-}4S]^{2+}$ spectrum (10%) to the least-squares fit of the $[2Fe\text{-}2S]^{2+}$ spectrum.

Resonance Raman Characterization of the $[4Fe\text{-}4S]^{2+}$ Center Assembled in IscU. Both resonance Raman and Mössbauer studies confirm the characterization of fraction 4 as a homogeneous $[4Fe\text{-}4S]^{2+}$-containing form of IscU. The resonance Raman spectrum (Figure 3) is uniquely indicative of a $[4Fe\text{-}4S]^{2+}$ center (*36*) and is dominated by the totally symmetric breathing mode of the [4Fe-4S] core at 343 cm^{-1}. Since the resonance enhancement of the Fe−S stretching modes in the Raman spectra of $[2Fe\text{-}2S]^{2+}$ centers is approximately 5-fold greater than for $[4Fe\text{-}4S]^{2+}$ clusters with 457 nm excitation (*36*), the absence of bands indicative of the $[2Fe\text{-}2S]^{2+}$ centers in IscU shows that fraction 4 is a homogeneous $[4Fe\text{-}4S]^{2+}$-containing form of IscU. Moreover, all the observed bands can be rationally assigned by direct analogy with the detailed vibrational assignments that have been made for model complexes and ferredoxins on the basis of extensive isotope shift data and normal mode calculations (*36*, *37*). The frequency of the totally symmetric breathing mode of the [4Fe-4S] core has been found to be a useful indicator of coordination by a noncysteinyl ligand at a unique Fe site of a $[4Fe\text{-}4S]^{2+}$ cluster (*27*, *38*). The currently observed ranges are 333−339 cm^{-1} for complete cysteinyl ligation and 340−343 cm^{-1} for clusters with OH$^-$, serinate, or aspartate ligation at a unique Fe site (*27*). By this criterion, the single $[4Fe\text{-}4S]^{2+}$ cluster in IscU is likely to have noncysteinyl ligation at one Fe site, and therefore could be located exclusively within one subunit or bridging subunits using ligands from both subunits.

Mössbauer Characterization of the $[4Fe\text{-}4S]^{2+}$ Center Assembled in IscU. The Mössbauer spectrum of fraction 4 recorded at 4.2 K in a parallel magnetic field of 50 mT exhibits a slightly asymmetric quadrupole doublet (Figure 4C). The solid line plotted over the data is the result of a least-squares fit to the data assuming two unresolved quadrupole doublets of equal intensity. The parameters obtained are listed in Table 1 and are typical for $[4Fe\text{-}4S]^{2+}$ clusters (*34*, *39*, *40*). Studies of $[4Fe\text{-}4S]^{2+}$ model compounds with tetrahedral coordinate Fe sites having mixed terminal ligands (thiophenolate and/or phenolate) indicate that the Mössbauer parameters are relatively insensitive to the nature of the ligand type (*41*). Figure 4E shows a spectrum of this sample recorded at 4.2 K in a parallel field of 4 T. The solid line plotted over the experimental spectrum is a theoretical simulation using the parameters obtained from the least-squares fit of the weak-field spectrum and assuming diamagnetism. The agreement between the experiment and simulation indicates that the cluster has a diamagnetic ground state as expected for a $[4Fe\text{-}4S]^{2+}$ cluster.

DISCUSSION

Our working hypothesis for Fe−S cluster biosynthesis is that the IscU protein provides a scaffold for IscS-directed

assembly of clusters that can be inserted intact into apo forms of Fe−S cluster-containing proteins, possibly via other associated carrier proteins (*11*, *12*). While intact cluster transfer from IscU has yet to be demonstrated, this hypothesis is further supported by the ability of IscU to accommodate both $[2Fe\text{-}2S]^{2+}$ and $[4Fe\text{-}4S]^{2+}$ clusters as evidenced by the UV−visible absorption, resonance Raman, and Mössbauer studies presented herein. Moreover, it is clear that IscS-mediated cluster assembly in IscU proceeds in sequential steps involving well-defined forms of IscU containing one $[2Fe\text{-}2S]^{2+}$ cluster per dimer, two $[2Fe\text{-}2S]^{2+}$ clusters per dimer, and one $[4Fe\text{-}4S]^{2+}$ cluster per dimer. The rates at which these individual species appear are critically dependent on the IscU:IscS ratio, and the reaction proceeds rapidly to yield the $[4Fe\text{-}4S]^{2+}$ cluster form in less than 1 h when a 1:1 IscU:IscS ratio is used. IscU and IscS have been shown to form a 1:1 complex (*12*). However, it is clearly premature to draw any conclusions concerning which of the cluster-containing forms of IscU that can be produced in vitro are physiologically relevant.

The $[2Fe\text{-}2S]^{2+}$ clusters in both the one- and two-$[2Fe\text{-}2S]^{2+}$ cluster-containing forms of IscU have been shown by the combination of UV−visible absorption, resonance Raman, and Mössbauer spectroscopies to have very similar protein environments with at least one and possibly two oxygen (nontyrosyl) or nitrogen (nonhistidyl) ligands at one Fe site. Since IscU has three conserved cysteine residues, each subunit can therefore accommodate one $[2Fe\text{-}2S]^{2+}$ cluster. However, the possibility that both $[2Fe\text{-}2S]^{2+}$ clusters bridge subunits cannot be excluded at this stage, and the observation that one of the two $[2Fe\text{-}2S]^{2+}$ clusters is selectively removed by EDTA treatment clearly merits further investigation. The ligation and subunit location of the $[4Fe\text{-}4S]^{2+}$ cluster in IscU are less well defined. The resonance Raman properties are best interpreted in terms of three cysteinyl ligands and one oxygenic ligand, but the possibility of complete cysteinyl ligation with anomalous Fe−S vibrational frequencies resulting from differences in H-bonding and/or $Fe-S_{\gamma}-C_{\beta}-C_{\alpha}$ dihedral angles, compared to those of other biological $[4Fe\text{-}4S]^{2+}$ centers, cannot be ruled out. In either case, the single $[4Fe\text{-}4S]^{2+}$ cluster in IscU could be located within one subunit or bridging between subunits.

The results also offer some insight into the mechanism of assembly of a [4Fe-4S] cluster in IscU. The conversion of the form of IscU containing two $[2Fe\text{-}2S]^{2+}$ clusters per dimer to the form containing one $[4Fe\text{-}4S]^{2+}$ cluster per dimer occurs in the absence of apoprotein and without an increase in the level of the apoprotein fraction (fraction 1) or the one-$[2Fe\text{-}2S]^{2+}$ cluster-containing fraction (fraction 2). Furthermore, it is not accompanied by the appearance of an IscU fraction containing one $[2Fe\text{-}2S]^{2+}$ and one $[4Fe\text{-}4S]^{2+}$ cluster or two $[4Fe\text{-}4S]^{2+}$ clusters. These observations argue against mechanisms for $[4Fe\text{-}4S]^{2+}$ cluster assembly involving degradation of $[2Fe\text{-}2S]^{2+}$ clusters and reassembly of a $[4Fe\text{-}4S]^{2+}$ cluster in apo IscU or building onto individual $[2Fe\text{-}2S]^{2+}$ clusters. Rather, the data are most consistent with a concerted [4Fe-4S] cluster assembly process with reductive conversion of two $[2Fe\text{-}2S]^{2+}$ clusters to one $[4Fe\text{-}4S]^{2+}$ cluster. Reductive coupling of two $[2Fe\text{-}2S]^{2+}$ clusters has long been known to be a viable approach for synthesizing $[4Fe\text{-}4S]^{2+}$ clusters in aprotic media (*42*). The work presented here provides the first evidence that this type of chemistry might be used in a general pathway of $[4Fe\text{-}4S]^{2+}$ cluster biosynthesis.

ACKNOWLEDGMENT

We thank Chad Williamson for technical help in the purification of proteins and Marly Eidsness in the BioXpress Laboratory at the University of Georgia for providing the mono-Q column and for advice on separating protein fractions.

REFERENCES

1. Beinert, H., Holm, R. H., and Münck, E. (1997) *Science 277*, 653−659.
2. Johnson, M. K. (1998) *Curr. Opin. Chem. Biol. 2*, 173−181.
3. Beinert, H., and Kiley, P. J. (1999) *Curr. Opin. Chem. Biol. 3*, 152−157.
4. Beinert, H. (2000) *J. Biol. Inorg. Chem. 5*, 2−15.
5. Dean, D. R., Bolin, J. T., and Zheng, L. (1993) *J. Bacteriol. 1756*, 6737−6744.
6. Zheng, L., and Dean, D. R. (1994) *J. Biol. Chem. 269*, 18723−18726.
7. Zheng, L., White, R. H., Cash, V. L., Jack, R. F., and Dean, D. R. (1993) *Proc. Natl. Acad. Sci. U.S.A. 90*, 2754−2758.
8. Zheng, L., White, R. H., Cash, V. L., and Dean, D. R. (1994) *Biochemistry 33*, 4714−4720.
9. Fu, W., Jack, R. F., Morgan, T. V., Dean, D. R., and Johnson, M. K. (1994) *Biochemistry 33*, 13455−13463.
10. Agar, J. N., Yuvaniyama, P., Jack, R. F., Cash, V. L., Smith, A. D., Dean, D. R., and Johnson, M. K. (2000) *J. Biol. Inorg. Chem. 5*, 167−177.
11. Yuvaniyama, P., Agar, J. N., Cash, V. L., Johnson, M. K., and Dean, D. R. (2000) *Proc. Natl. Acad. Sci. U.S.A. 97*, 599−604.
12. Agar, J. N., Zheng, L., Cash, V. L., Dean, D. R., and Johnson, M. K. (2000) *J. Am. Chem. Soc. 122*, 2136−2137.
13. Zheng, L., Cash, V. L., Flint, D. H., and Dean, D. R. (1998) *J. Biol. Chem. 273*, 13264−13272.
14. Flint, D. H. (1996) *J. Biol. Chem. 271*, 16068−16074.
15. Fujii, T., Maeda, M., Mihara, H., Kurihara, T., Esaki, N., and Hata, Y. (2000) *Biochemistry 39*, 1263−1273.
16. Kaiser, J. T., Clausen, T., Bourenkow, G. P., Bartunik, H.-D., Steinbacher, S., and Huber, R. (2000) *J. Mol. Biol. 297*, 451−464.
17. Hwang, D. M., Dempsey, A., Tan, K. T., and Liew, C. C. (1996) *J. Mol. Evol. 43*, 536−540.
18. Kispal, G., Csere, P., Prohl, C., and Lill, R. (1999) *EMBO J. 18*, 3981−3989.
19. Schilke, B., Voisine, C., Beinert, H., and Craig, E. (1999) *Proc. Natl. Acad. Sci. U.S.A. 96*, 10206−10211.
20. Strain, J., Lorenz, C. R., Bode, J., Garland, S., Smolen, G. A., Ta, D. T., Vickery, L. E., and Culotta, V. C. (1998) *J. Biol. Chem. 273*, 31138−31144.
21. Land, T., and Rouault, T. A. (1998) *Mol. Cell 2*, 807−815.
22. Smith, P. K., Krohn, R. L., Hermanson, G. T., Mallia, A. K., Gartner, F. H., Provenzano, M. D., Fujimoto, E. K., Goeke, N. M., Olson, B. J., and Klenk, D. C. (1985) *Methods Enzymol. 226*, 199−232.
23. Ravi, N., Bollinger, J. M., Jr., Huynh, B. H., Stubbe, J., and Edmondson, D. E. (1994) *J. Am. Chem. Soc. 116*, 8007−8014.
24. Fawcett, S. E. J., Davis, D., Breton, J. L., Thomson, A. J., and Armstrong, F. A. (1998) *Biochem. J. 335*, 357−368.
25. Dailey, H. A., Finnegan, M. G., and Johnson, M. K. (1994) *Biochemistry 33*, 403−407.
26. Johnson, M. K., Robinson, A. E., and Thomson, A. J. (1982) in *Iron−Sulfur Proteins* (Spiro, T. G., Ed.) pp 367−406, Wiley-Interscience, New York.
27. Brereton, P. S., Duderstadt, R. E., Staples, C. S., Johnson, M. K., and Adams, M. W. W. (1999) *Biochemistry 38*, 10594−10605.

28. Crouse, B. R., Sellers, V. M., Finnegan, M. G., Dailey, H. A., and Johnson, M. K. (1996) *Biochemistry 35*, 16222−16229.
29. Wu, C.-K., Dailey, H. A., Rose, J. P., Burden, A., and Wang, B.-C. (2000) *Nat. Struct. Biol.* (in press).
30. Kuila, D., Schoonover, J. R., Dyer, R. B., Batie, C. T., Ballou, D. P., Fee, J. A., and Woodruff, W. H. (1992) *Biochim. Biophys. Acta 1140*, 175−183.
31. Que, L., Jr. (1988) in *Biological Applications of Raman Spectroscopy. Vol. 3: Resonance Raman Spectra of Heme and Metalloproteins* (Spiro, T. G., Ed.) pp 491−521, Wiley-Interscience, New York.
32. Yoo, S. J., Angove, H. C., Burgess, B. K., Hendrich, M. P., and Münck, E. (1999) *J. Am. Chem. Soc. 121*, 2534−2545.
33. Fee, J. A., Findling, K. L., Yoshida, T., Hille, R., Tarr, G. E., Hearshen, D. O., Dunham, W. R., Day, E. P., Kent, T. A., and Münck, E. (1984) *J. Biol. Chem. 259*, 124−133.
34. Trautwein, A. X., Bill, E., Bominaar, E. L., and Winkler, H. (1991) *Struct. Bonding 78*, 1−95.
35. Iwata, S., Saynovits, S., Link, T. A., and Michel, H. (1996) *Structure 4*, 567−579.
36. Spiro, T. G., Czernuszewicz, R. S., and Han, S. (1988) in *Biological Applications of Raman Spectroscopy. Vol. 3: Resonance Raman Spectra of Heme and Metalloproteins* (Spiro, T. G., Ed.) pp 523−554, Wiley-Interscience, New York.
37. Czernuszewicz, R. S., Macor, K. A., Johnson, M. K., Gewirth, A., and Spiro, T. G. (1987) *J. Am. Chem. Soc. 109*, 7178−7187.
38. Conover, R. C., Kowal, A. T., Fu, W., Park, J.-B., Aono, S., Adams, M. W. W., and Johnson, M. K. (1990) *J. Biol. Chem. 265*, 8533−8541.
39. Middleton, P., Dickson, D. P. E., Johnson, C. E., and Rush, J. D. (1978) *Eur. J. Biochem. 88*, 135−141.
40. Middleton, P., Dickson, D. P. E., Johnson, C. E., and Rush, J. D. (1980) *Eur. J. Biochem. 104*, 289−296.
41. Kanatzidis, M. G., Baenziger, N. C., Coucouvanis, D., Simopoulos, A., and Kostikas, A. (1984) *J. Am. Chem. Soc. 106*, 4500−4511.
42. Hagen, K. S., Reynolds, J. G., and Holm, R. H. (1981) *J. Am. Chem. Soc. 103*, 4054−4063.

BI000931N